applied sciences

MDPI

Article

Investigation on Deformation Behavior of the Crossing Section of Two Municipal Road Tunnels during Construction

Chen-Yu Zhao [1], Ren-Hui Yue [2], Yu-Liang Lin [1,*], Cong-Jun Huang [2] and Xu Jiang [2]

[1] School of Civil Engineering, Central South University, Changsha 410075, China
[2] Hefei Urban Planning & Design Institute, Hefei 230041, China
* Correspondence: linyuliang11@163.com

Abstract: With the development of urbanization, the transportation network of underground tunnels has been gradually formed and improved. It is a complicated issue for engineering construction when two municipal road tunnels intersect at one point. Based on a construction site of the crossing point of the Huayuan Road Tunnel and Luzhou Road Tunnel in Hefei City, China, the finite element analysis method is used to calculate and analyze the deformation characteristics of the crossing point of the tunnels during the asymmetric construction of connecting parts. The deformation behaviors of the crossing point of tunnels subjected to symmetrical construction are also studied for comparison. Results show that the deformations of the supporting pile and tunnel frame structures increase rapidly when they are subjected to asymmetric construction, while the lateral movement of the supporting pile and the deformation of the tunnel structure can be greatly limited when the symmetrical construction method is adopted. Some suggestions for engineering construction are put forward to ensure the safety of the structure, such as multi-stage construction and temporary supporting measure.

Keywords: orthogonal tunnel; numerical simulation; asymmetric excavation; symmetrical excavation; pit

Citation: Zhao, C.-Y.; Yue, R.-H.; Lin, Y.-L.; Huang, C.-J.; Jiang, X. Investigation on Deformation Behavior of the Crossing Section of Two Municipal Road Tunnels during Construction. *Appl. Sci.* **2022**, *12*, 12274. https://doi.org/10.3390/app122312274

Academic Editor: Syed Minhaj Saleem Kazmi

Received: 28 October 2022
Accepted: 28 November 2022
Published: 30 November 2022

1. Introduction

With the rapid development of China's economy, the urban population has increased significantly and traffic has become more and more saturated. Multiple three-dimensional underground transportation systems have been established in order to relieve the traffic pressure in many cities. With regard to the construction of such systems, foundation pits are constructed near the existing tunnel structure that may induce mechanical interference against the safety of the structure.

The effects of the surrounding excavation on the tunnel structure can be studied by theoretical analysis, experimental methods and numerical simulation. Klar et al. [1] compared the elastic continuum solution with a closed-form Winkler solution with Vesic subgrade modulus while analyzing the influence of tunneling on existing pipelines. Vorster et al. [2] presented a method for estimating the maximum bending moment of the pipeline caused by tunneling. Zhang et al. [3] presented a semi-analytical method to estimate the uplifts of an adjacent tunnel during deep excavation. Zhang et al. [4,5] presented a two-stage method to calculate the deformation of a tunnel caused by adjacent excavation. Liang et al. [6,7] used the two-stage method to study the interaction between tunnels and excavation, and the tunnel–ground interaction when using a Pasternak foundation beam was analyzed. Han et al. [8] assumed the existing tunnels as having a beam on a Winkler elastic foundation and calculated the deformation and internal force of the tunnel structure by a singular function. Sun et al. [9] presented the analytical model for estimating the tunnel deformation caused by a square excavation based on Mindlin's solutions. Xu et al. [10] presented a semi-empirical formula for estimating the displacement of tunnels during adjacent excavation by statistical analysis.

Experimental study is an effective method to reveal the mechanical behavior of a geotechnical structure [11–15]. In particular, the field test results are generally regarded as the most valuable first-hand information [16]. Chang et al. [17] studied the response of the Taipei Rapid Transit System Tunnel caused by adjacent excavation, which was a reference for the establishment of an excavation standard. Sharma et al. [18] monitored the deformation of the Mass Rapid Transit tunnel during a large excavation nearby, and the influence of the stiffness of the tunnel lining on the displacement and distortion was discussed. Chen et al. [19] investigated the influence of a nearby excavation in soft soils on the existing Ningbo Metro Line 1 tunnels through field monitoring. Meng et al. [20] focused on engineering measures to reduce the effect of adjacent excavation via three groups of centrifuge tests. Chen et al. [21] conducted several centrifuge tests on the interaction between adjacent foundation pits with an aim to provide some suggestions for reducing the adjacent excavation effect.

The model geometry and model parameters can be easily changed as required in numerical analysis. Consequently, numerical simulation is regarded as a powerful and economical method to reveal the mechanical behavior of a geotechnical structure [22–24]. Zhang et al. [25] established a pipe–soil coupling model to investigate the excavation effect of a foundation pit adjacent to a hydrogen pipe. Zhou et al. [26] investigated the effects of unilateral excavation near a metro station, and a physical model test and discrete element method were adopted to analyze the influence of station width and excavation depth. Wang et al. [27] evaluated the tunnel deformation law and soil stress distribution by hypo-plastic model analysis under different excavation locations of foundation pits. Yang et al. [28] studied the deep excavation behavior of a pit adjacent to a flexible retaining wall, and the influences of excavation depth, wall depth and bending rigidity on the mechanical behavior of a retaining wall were studied by numerical simulation. Liu et al. [29] sought the best supporting measure for a foundation pit that enhanced the stability of adjacent tunnels based on a simulation of the whole excavation process. Chen et al. [30] established a 3-D numerical model to study the effect of triangular-distribution tunnel excavation on surface settlement and tunnel stability.

The above research works are beneficial to the development of tunnel construction technology. However, the geological conditions of engineering vary greatly from site to site. Moreover, few studies have been carried out with respect to the tunnel crossing section, which is regarded as a more complicated condition. In this study, an analysis model of the crossing section of two municipal road tunnels is established by using the ABAQUS finite element platform based on a construction project of the Huayuan Road Tunnel and Luzhou Road Tunnel in Hefei City, China. Two construction measures (i.e., symmetrical and asymmetrical construction processes) are designed to investigate the deformation behavior of the crossing section during the construction of the connecting part for comparison.

2. Background

Huayuan Road and Luzhou Road are two main municipal roads in Hefei City, China, and they were both constructed in the form of open tunnel. The open trench tunnel of Huayuan Road is 2.9 km in length, ranging from Huizhou Road to Baohe Road, which is crossed by the Luzhou Road Tunnel, as shown in Figure 1. To make the construction of this crossing section of the road tunnels workable, a combined box culvert was adopted where a frame structure of the Huayuan Road Tunnel downward side was combined with an upward side frame structure of the Luzhou Road Tunnel. The crossing section was named as the "Huayuan-Luzhou" Crossing Point. The physical dimension of the Huayuan Road pit was about 35 m wide and 20 m deep, which was partly supported by a cast-in-place pile (supporting pile) or by natural sloping. The pit of Luzhou Road was excavated shallowly by natural sloping near the two sides of Huayuan Road. Figure 2 shows the two orthogonal sections of the "Huayuan-Luzhou" Crossing Point.

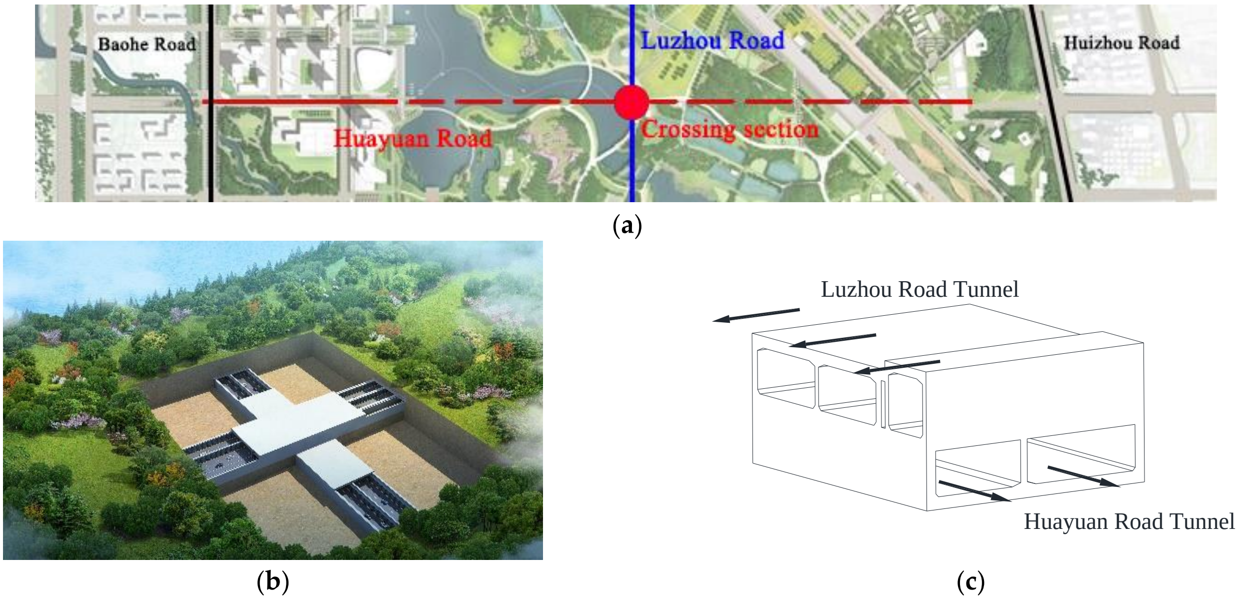

Figure 1. Location and structural diagram of the crossing section of Huayuan Road and Luzhou Road: (**a**) plane layout, (**b**) three-dimensional location diagram of crossing section and (**c**) structural frame diagram of crossing section.

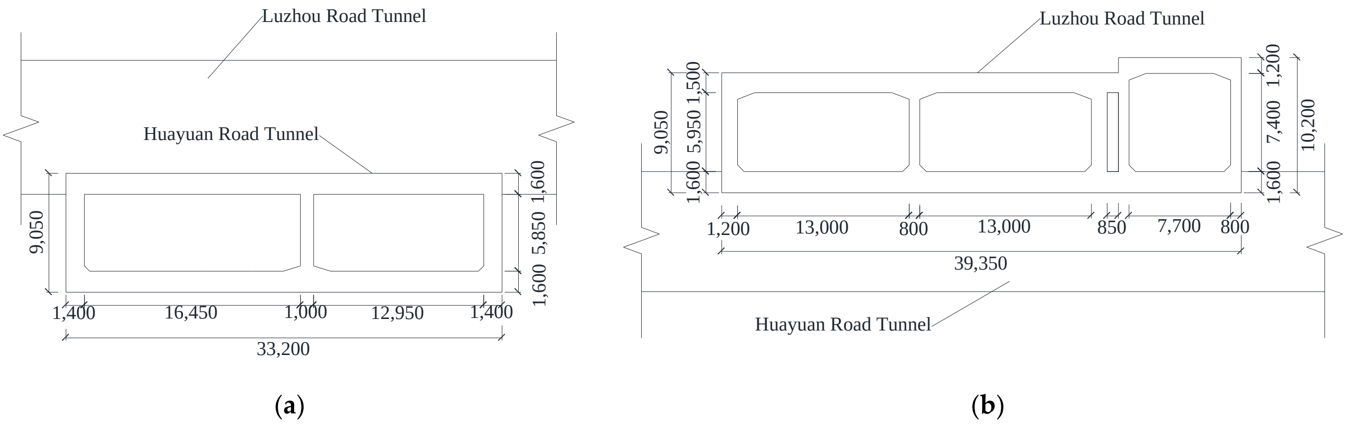

Figure 2. Two orthogonal sections of "Huayuan-Luzhou" Crossing Point: (**a**) Huayuan Road and (**b**) Luzhou Road (unit: mm).

The tunnel frame structure of Huayuan Road was constructed prior to that of Luzhou Road (see Figure 3). Consequently, the mechanical behavior of the tunnel frame structure of Huayuan Road was greatly affected by the construction of Luzhou Road as it approached the crossing section. In engineering the crossing point, the construction process of such a long tunnel was carried out from one section to another (about 25 m in length per section), and the section next to the Huayuan Road foundation pit was regarded as a connecting section that served as a connection of the Huayuan Road Tunnel and Luzhou Road Tunnel. The deformation behavior of the crossing section is a main issue for engineering the construction. In order to study the influence of the construction process on the deformation behavior of the connecting section, the whole construction process was divided into six procedures, as shown in Figure 3. Firstly, the pit of Huayuan Road around the crossing section was excavated and supported by a series of cast-in-place piles and three-row transverse support. Secondly, the tunnel frame structure of the crossing section was constructed from the bottom to the top (Huayuan Road downward sides and Luzhou Road upward sides). Thirdly, the southern pit of the connecting section was excavated in the Huayuan Road Tunnel, and the soil behind the supporting pile was removed in two steps according to the construction scheme (as shown in Figure 4). Fourthly, the part of the supporting pile above the pit bottom was cut off. Fifthly, the upper tunnel frame structure of the connecting section (tunnel frame structure of Luzhou Road) was constructed. Finally, the tunnel frame structure of the connecting section at the northern part was constructed the same way as the southern part.

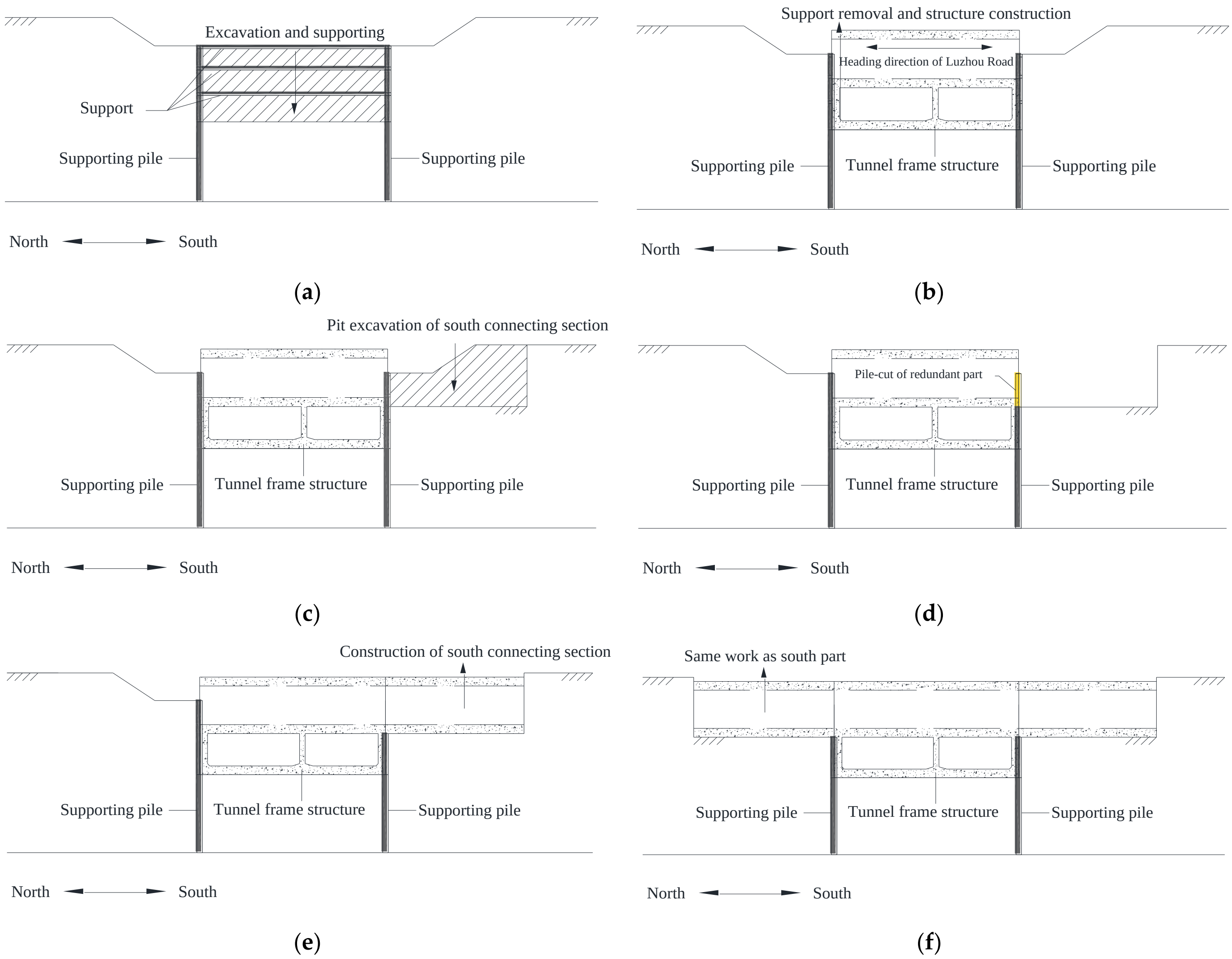

Figure 3. Construction process of connecting section: (**a**) pit excavation with supporting pile in Huayuan Road; (**b**) construction of frame structure in Huayuan Road; (**c**) excavation of pit in southern connecting part; (**d**) supporting pile cutting; (**e**) construction of southern connecting frame structure and (**f**) construction of northern connecting frame structure.

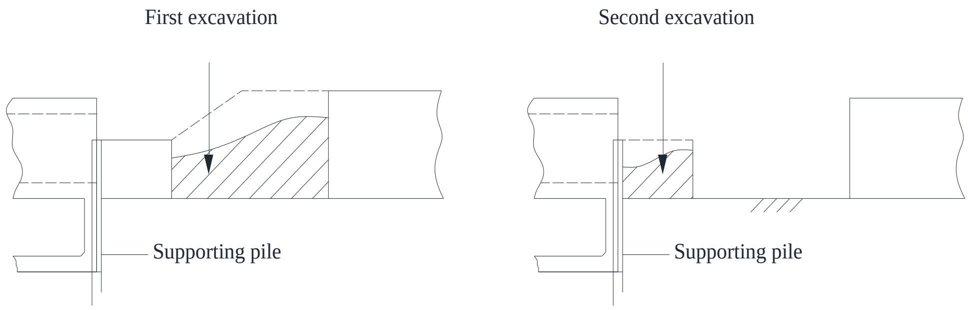

Figure 4. Excavation of foundation pit behind supporting pile.

Based on the construction process of the connecting section (see Figure 3), it can be seen that an asymmetric construction measure was adopted in the engineering, since the soil excavation of the foundation pit in the southern part was conducted prior to the soil excavation in the northern part. Large structure deformation and soil settlement might occur because of a sudden stress release and an unevenly distributed loading during asymmetric construction [31,32]. The asymmetric construction measure might result in a structural deflection and subsequently affect the function of the tunnel structure.

3. Numerical Model and Analysis Method

3.1. Numerical Model

The deformation behavior of the crossing section of the Huyuan Road Tunnel and Luzhou Road Tunnel can be effectively obtained by means of numerical simulation, and the construction conditions can be changed as required. According to the construction process of the Huayuan Road Tunnel, a 3-D numerical model was established to simulate the asymmetric construction process of the crossing section with the help of the ABAQUS finite element platform, and the deformation behaviors of the tunnel structure and supporting pile were analyzed. The foundation pit of Huayuan Road was 33.2 m in width and 39.4 m in length with a slope excavation depth of 5 m and a pit excavation depth of 13.4 m. The pits on the two sides of Luzhou Road around the connecting section were both 25.0 m in width with an excavation depth of 10.9 m. The numerical model and mesh generation are shown in Figure 5. The numerical model constituted 75,969 elements and 100,728 nodes. The models of the supporting pile, the frame structure of the tunnel and the surrounding soil were all established by an eight-node brick element. The bottom of the numerical model was fixed at x, y and z directions, and the lateral sides of the model were fixed at x and y directions. The free field was adopted to deal with the model boundary.

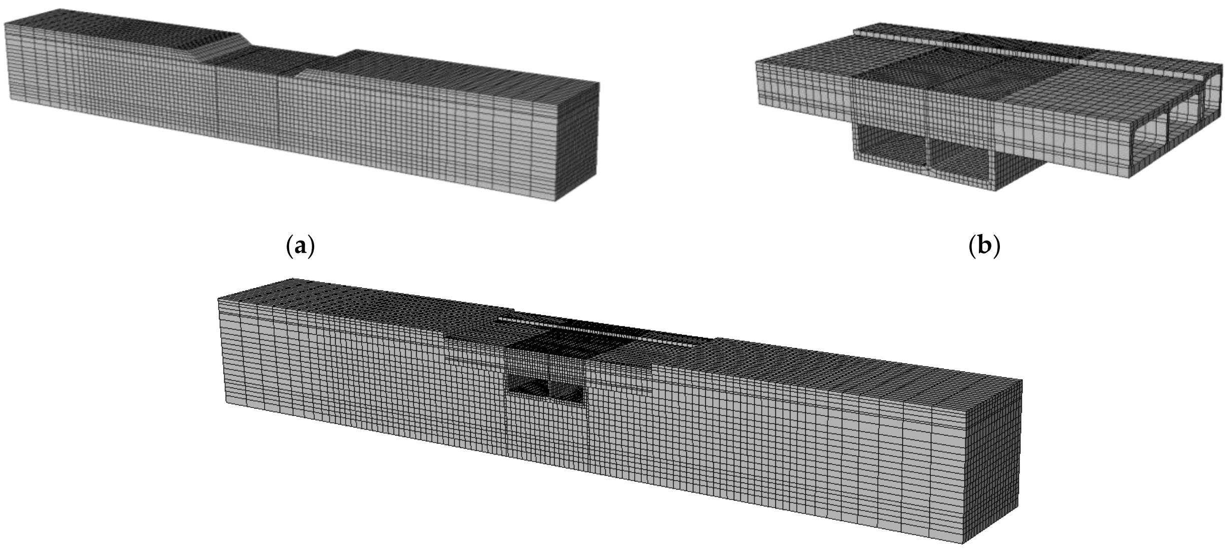

(**a**) (**b**) (**c**)

Figure 5. Numerical model of tunnel frame structure of Huayuan Road: (**a**) solid model; (**b**) tunnel model; (**c**) entire model.

3.2. Constitutive Model and Parameters

The soil was simulated with the M-C model, and the physical and mechanical properties of the soil were obtained based on the manual of engineering geology and reconnaissance report, as shown in Table 1. The frame structures of the tunnel and the supporting pile were constructed with reinforced concrete, and they were simulated with the elastic model. The mechanical parameters of the concrete structure are shown in Table 2. The interactions were set among the soil, the tunnel structure and the supporting piles with a friction coefficient of 0.3.

Table 1. Parameters of soil layer.

Layer ID	Soil Layer	Unit Weight/γ (kN·m^{-3})	Elastic Modulus/E (MPa)	Poisson Ratio/ν	Internal Friction Angle/ϕ (°)	Cohesive (kPa)
①	Miscellaneous fill	18.5	21	0.3	10.0	5.0
②	Clay	19.2	33	0.3	15.0	81.2
③	Clay	19.2	42	0.28	15.6	88.9
④	Silty clay	19.1	36	0.27	18.0	26.7
⑤	Clay	19.3	48	0.28	15.8	97.0
⑥	Silty clay with silt	20.0	36	0.3	25.0	20.0
⑦	Argillaceous sandstone strongly weathered	20.5	48	0.3	30.0	28.0

Remarks: There are 7 soil layers, and they are numbered as Layer ID ①~⑦.

Table 2. Parameters of concrete material.

Unit Weight/γ (kN·m^{-3})	Elastic Modulus/E (MPa)	Poisson Ratio/ν
26.0	3.15×10^4	0.2

3.3. Construction Procedure in Numerical Analysis

The main construction steps of the actual construction were reflected by 9 construction cases in numerical simulation in order to investigate the deformation behavior caused by asymmetrical construction. For a comparison, an additional case of symmetrical construction was designed with the same engineering parameters attached. The processes for asymmetrical construction and symmetrical construction are summarized in Table 3, in which the process of asymmetrical construction is summarized in Cases 1~9, and the process of symmetrical construction is divided into Cases 1~5. The above cases cover the key construction procedures of the connecting section when the asymmetrical or symmetrical construction method is adopted. The deformation behaviors the of tunnel frame structure and supporting pile were investigated with the aim of providing some suggestions for a reasonable engineering scheme in deformation control.

Table 3. Procedure of asymmetrical and symmetrical construction.

Asymmetrical Construction		Symmetrical Construction	
Cases	Procedure	Cases	Procedure
1	Construction of crossing point	1	Construction of crossing point
2	First soil excavation behind southern piles	2	First soil excavation behind pile on both sides
3	Second soil excavation behind southern piles	3	Second soil excavation behind pile on both sides
4	Southern pile cut	4	Pile cut
5	Construction of southern connecting section	5	Construction of northern connecting section
6	First soil excavation behind northern piles		
7	Second soil excavation behind northern piles		
8	Northern pile cut		
9	Construction of northern connecting section		

3.4. Valuation of Numerical Model

In order to verify the effectiveness of numerical simulation, the numerical results of the axial strain of the top slab were compared with those observed in the field investigation of several cases (Cases 2–4) in asymmetrical construction, as shown in Figure 6. The numerical simulation captured the basic changing regulation of the axial strain of the top slab, and it showed a decreasing tendency along its width. Meanwhile, the value of axial strain in numerical simulation is quite close to that in field investigation. Consequently, it is regarded that the results determined by numerical simulation are consistent with those obtained by field investigation.

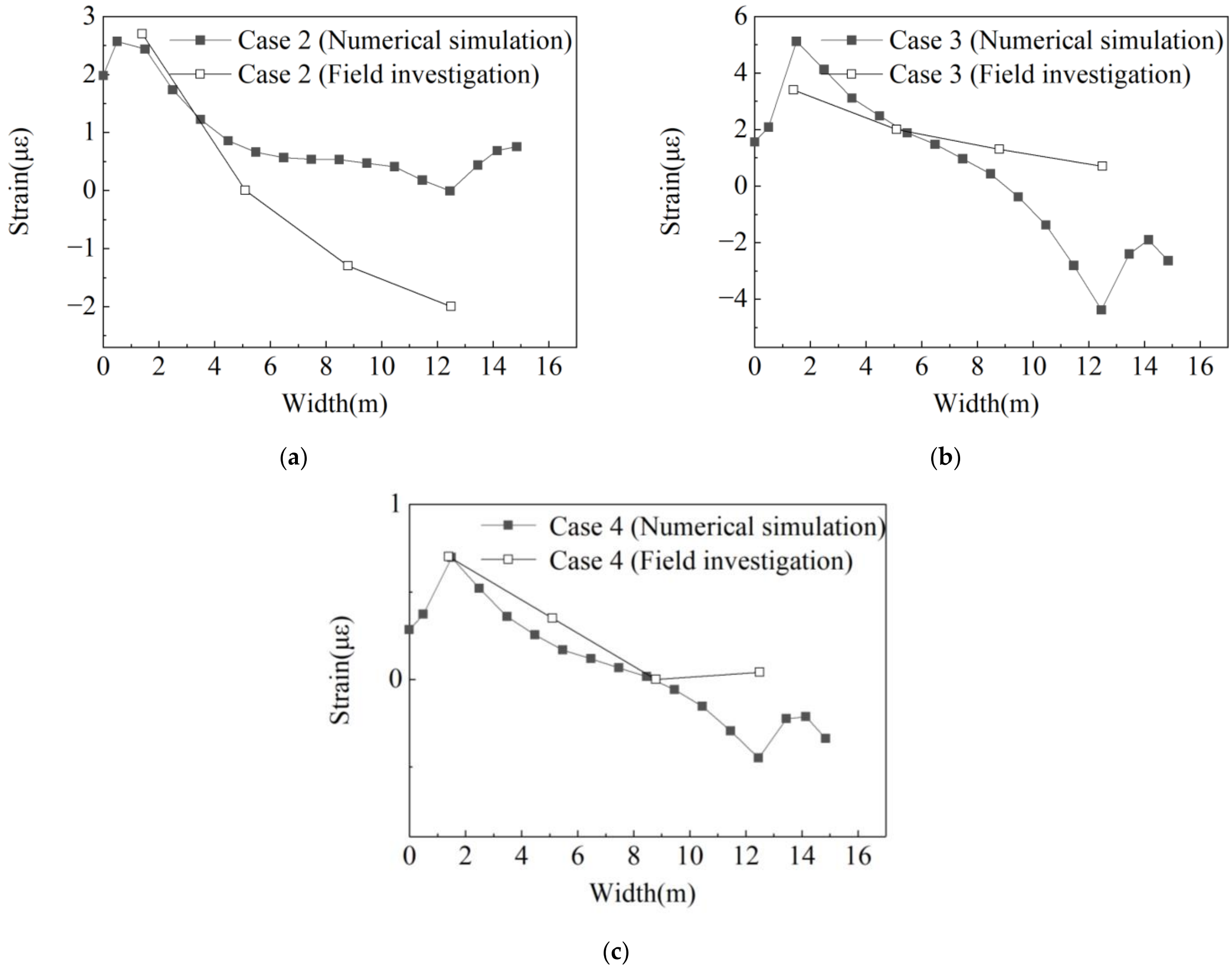

Figure 6. Comparisons of strain of top slab between numerical simulation and field investigation: (**a**) Case 2; (**b**) Case 3 and (**c**) Case 4 (unit: με).

4. Results and Analysis

4.1. Results of Asymmetrical Construction

4.1.1. Lateral Displacement of Supporting Pile

The displacement curves of supporting pile subjected to different construction processes are shown in Figure 7. It is seen that southern pile deforms obviously during the excavation of the southern pit. The displacement at the top of the pile is 3.48 mm towards the soil, and it is 7.11 mm at the bottom of pit after soil excavation. The maximum deformation is observed at the bottom of the pit. During the process of pile cutting above the pit bottom, little deformation is observed. When the construction of the southern connecting part is complete, the remaining part of the pile moves towards the opposite direction (away from the soil), with the maximum value of 4.98 mm at the top and 2.76 mm at the bottom. The deformation at the bottom decreases more obviously than that at the top. When the construction of the northern connecting section is completed, the deformation of the pile shows a similar change. During the whole procedure of asymmetric construction, the maximum deformation of the pile is 10.53 mm at the pit bottom, which indicates that the lateral displacement varies more significantly at the bottom of the pit.

A similar deformation behavior is observed in the northern pile, as shown in Figure 6b. During the construction of the southern part, the deformation of the supporting pile (towards the soil) is 4.13 mm at the top and 2.23 mm at the bottom. After construction, little deformation is observed below the pit bottom, with the maximum deformation of 1.98 mm at the pit bottom. During the whole construction procedure, the maximum lateral displacement towards the soil is 6.27 mm, which occurs at the pit bottom of the tunnel structure.

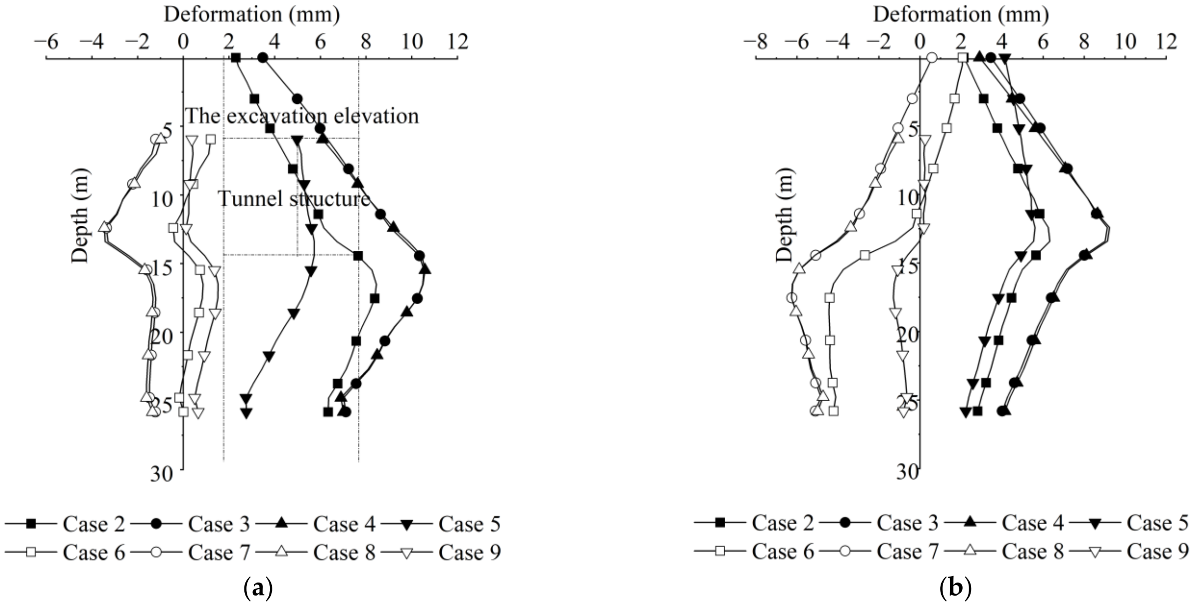

Figure 7. Lateral deformation of supporting pile by asymmetric construction method: (**a**) southern pile and (**b**) northern pile (unit: mm).

The above deformation behavior is related to the mechanical characteristics of the supporting pile (see Figure 8). The supporting pile is divided into two parts by taking the bottom line of the foundation pit as the interface, known as Section *AB* and Section *BC*. As for Section *AB*, the deformation behavior of the supporting pile is dependent on the loading cases. The supporting pile tends to move towards the direction away from foundation pit when the soil behind supporting pile is excavated. The construction of the tunnel frame structure on the other side will also cause the supporting pile to move away from the foundation pit. There is an uneven stress of the whole system, and the supporting pile is affected by earth pressure from the left side. As for the Section *BC*, the supporting pile tends to move towards the right during the whole construction period (see Figure 8), since there is a constraint at Section *AB* due to the tunnel frame structure. Section *BC* is extruded by the soil near the connection section due to the self-weight of the tunnel frame structure, as well as an unloading induced by soil excavation on the other side. The distribution of force greatly influences the deformation behavior of the supporting pile.

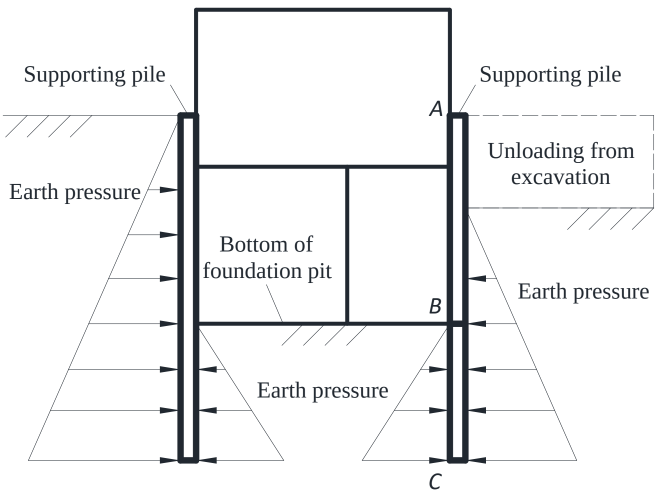

Figure 8. The force analysis of supporting pile.

4.1.2. Deformation of Tunnel Frame Structure

An analysis of the tunnel frame structure is shown in Figure 9 by taking the tunnel frame of the "Huayuan-Luzhou" Crossing Point as an example. Figure 10 shows the deformation curve of the bottom slab and top slab of the tunnel frame structure at the crossing point. The position of the middle wall in tunnel frame structure is set as the origin of the axial coordinate (see Figure 9). The bottom slab is floating during the asymmetric excavation of the connecting section. The maximum vertical deformation of the bottom slab occurs on the side next to the excavation position, and it is approximately 16 mm during the construction. The construction of the tunnel frame structure causes the slab settlement. At the end of construction, the vertical deformation tends to be stable, with a uniform value of about 6 mm. As for the top slab, the deformation behavior is similar to that of the bottom slab, which means there is little relative deformation between these two slabs.

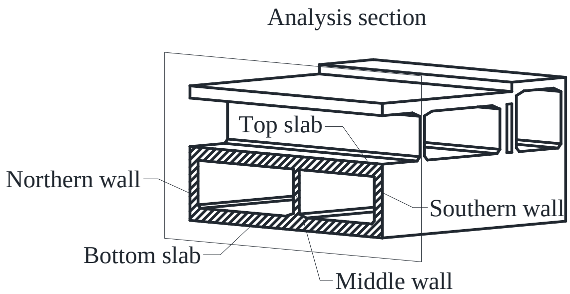

Figure 9. Typical analysis section of tunnel frame structure.

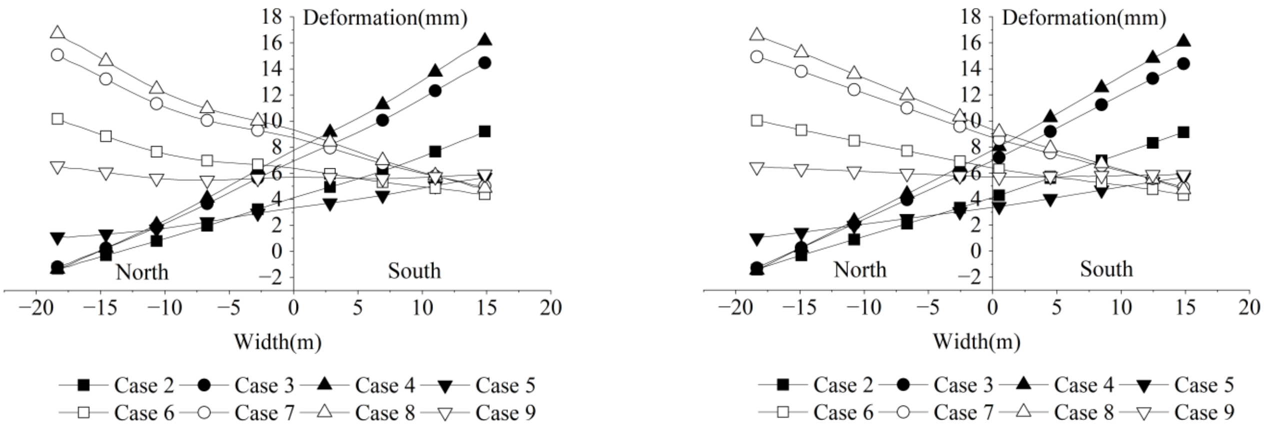

(**a**) (**b**)

Figure 10. Vertical deformation of structural slab subjected to asymmetric construction: (**a**) bottom slab and (**b**) top slab (unit: mm).

Figure 11 shows the deformation of the northern wall, middle wall and southern wall of the tunnel frame structure. The deformation behaviors of these structural walls are quite similar. A deformation towards the soil is observed at the structural walls with the maximum value at the bottom during an asymmetric excavation of the soil behind the supporting pile. Generally, the pile-cut-induced deformation of structural walls is slight and negligible. During the construction of the connecting section, the wall moves backward towards the soil and subsequently induces an inclination of the structural wall. The deformation of the structural wall is well controlled, and it turns vertical with an even value within 0.5 mm. The overall deformation trend of the structural wall is generally consistent with that of the supporting pile.

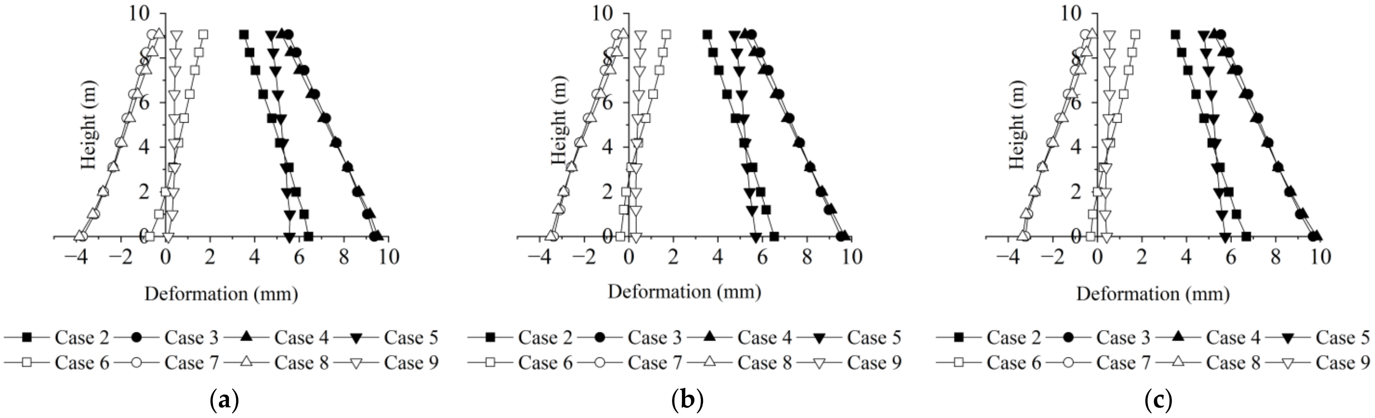

Figure 11. Lateral deformation of structural wall subjected to asymmetric construction: (**a**) northern wall, (**b**) middle wall and (**c**) southern wall (unit: mm).

4.2. Results of Asymmetrical Construction

Based on the above analysis, an uneven deformation is observed in the supporting pile and tunnel frame structure when the asymmetric construction method is adopted. To strictly limit the deformation of the tunnel frame structure during the construction process, a symmetric construction method is put forward. A symmetrical soil excavation with a simultaneous construction of a tunnel frame structure is adopted in symmetric construction, and the inclination deformation can be limited effectively as expected during the whole construction. Figure 12 shows the deformation of the supporting pile subjected to symmetric construction. The deformation of the supporting pile is mainly observed in Section *BC*, which is caused by the squeezing of soil, while Section *AB* is constrained by the tunnel frame structure, and no obvious deformation is observed. The maximum deformation of the southern supporting pile is 4.04 mm, and the deformation decreases after the construction of the connecting section with a residual deformation of 1.51 mm. The maximum deformation of the northern supporting pile is 4.14 mm after excavation, and the residual deformation is 1.62 mm after the construction of the connecting section.

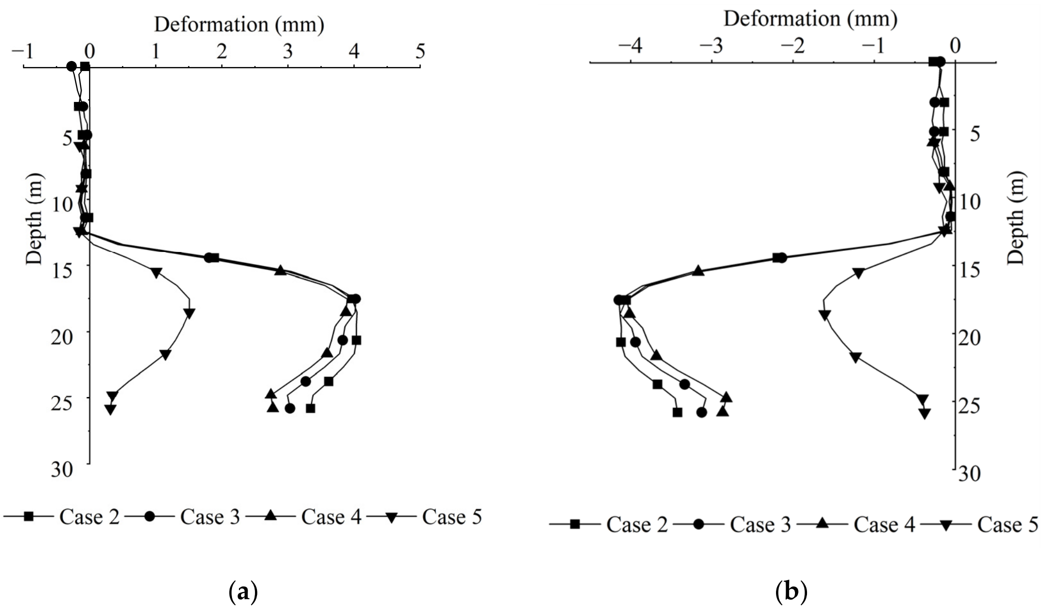

Figure 12. Lateral deformation of supporting pile subjected to symmetric construction: (**a**) southern pile and (**b**) northern pile (unit: mm).

Figures 13 and 14 show the deformation of the structural slab and structural wall in the tunnel frame structure subjected to symmetric construction. There is a uniform floating deformation of about 13 mm in the structural slab during the soil excavation case, and it increases by 1 mm after the pile cut and then drops to an even floating value of about 6 mm during the period of structure construction. Generally, the slabs deform uniformly when subjected to symmetric construction. As for the structural wall, the deformation is well controlled within 0.5 mm during the whole symmetric construction procedure. Such a small deformation is negligible in engineering practice.

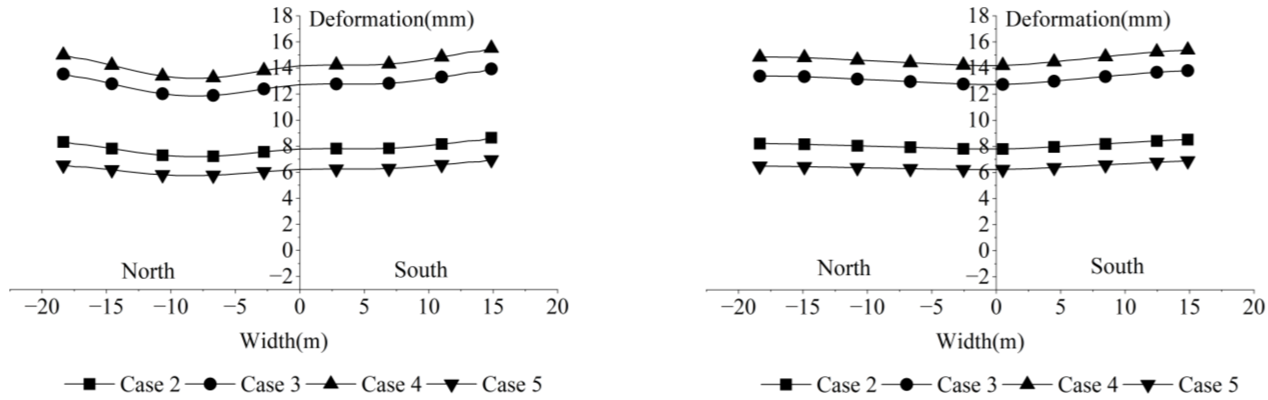

(**a**) (**b**)

Figure 13. Vertical deformation of structural slab subjected to symmetric construction: (**a**) bottom slab and (**b**) top slab (unit: mm).

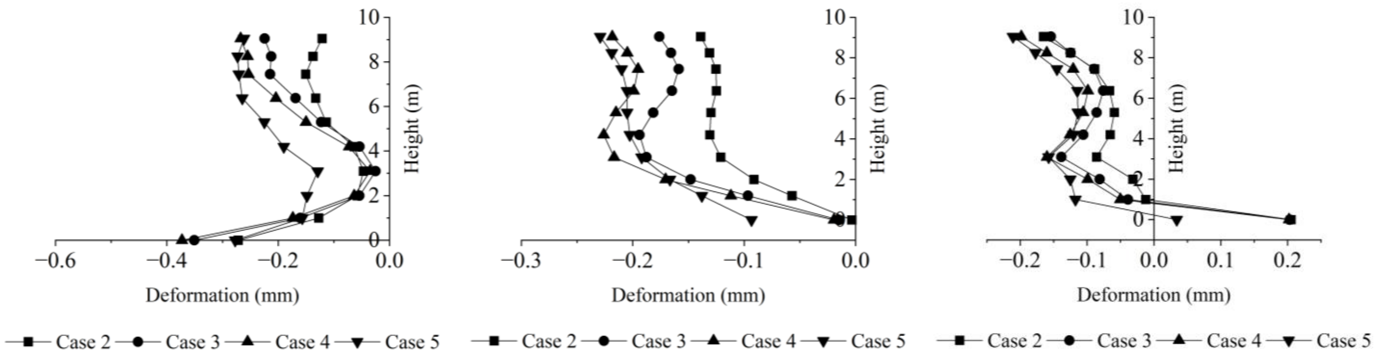

(**a**) (**b**) (**c**)

Figure 14. Lateral deformation of structural wall subjected to symmetric construction: (**a**) northern wall; (**b**) middle wall and (**c**) southern wall (unit: mm).

To ensure a positive function on deformation control in symmetrical construction, uniform and synchronous construction measures on both sides of the Huayuan foundation pit are necessary, and the adverse effects caused by the time–space effect should be reduced. For example, the excavation of the soil behind supporting pile should be carried out in symmetrical multiple steps. The construction procedure can be performed by an inverse method where the connecting structure is constructed from top to bottom right after the soil excavation to reduce the unloading effect caused by soil excavation.

5. Conclusions

In this paper, the deformation behavior of a tunnel crossing section subjected to symmetric and asymmetric construction is discussed. The deformation behaviors of the supporting pile and tunnel frame structure are analyzed.

An asymmetric construction method is adopted for the connecting section of two municipal road tunnels in engineering practice, resulting in a relatively large deformation due to unbalanced force. The maximum deformation of the supporting pile is 10.57 mm at the southern side and 6.27 mm at the northern side near the bottom of the pit subjected to soil excavation at the southern side. The bottom and top slabs of the tunnel frame structure are affected due to the soil unloading at the southern side, and the maximum values of floating in the bottom slab and top slab are 16.16 mm and 16.08 mm, respectively. The structural walls show the same deformation characteristics as the supporting pile nearby.

A symmetrical construction method is simulated for comparison, which can effectively reduce the impact on the existing structure at crossing point. The maximum deformation of the supporting pile is 4.04 mm at the southern side and 4.13 mm at the northern side subjected to symmetrical construction. As for the bottom slab and top slab, both of them float after construction with a uniform deformation value of about 14 mm. The deformation caused by symmetrical construction is much smaller compared with that induced by asymmetrical construction.

Deformation of the tunnel frame structure or supporting pile caused by asymmetric construction is much more obvious than that subjected to symmetric construction. A temporary supporting structure is recommended to be erected at the cantilever part of the supporting pile for asymmetric construction.

Author Contributions: Conceptualization, C.-Y.Z. and R.-H.Y.; methodology, C.-Y.Z.; software, C.-Y.Z.; validation, C.-Y.Z. and Y.-L.L.; formal analysis, C.-Y.Z.; investigation, C.-Y.Z. and R.-H.Y.; resources, R.-H.Y., C.-J.H. and X.J.; data curation, C.-Y.Z. and R.-H.Y.; writing—original draft preparation, C.-Y.Z. and Y.-L.L.; writing—review and editing, C.-Y.Z. and Y.-L.L.; visualization, C.-Y.Z. and Y.-L.L.; supervision, Y.-L.L.; project administration, R.-H.Y., C.-J.H. and X.J.; funding acquisition, R.-H.Y., C.-J.H. and X.J. All authors have read and agreed to the published version of the manuscript.

Funding: This research was funded by the Science and Technology Project of Urban and Rural Housing Construction of Anhui Province, China, grant number 2021-YF42 and the Hunan Provincial Natural Science Foundation of China, grant number 2021JJ30830.

Institutional Review Board Statement: Not applicable.

Informed Consent Statement: Not applicable.

Data Availability Statement: The data presented in this study may be available on reasonable request from the corresponding author.

Acknowledgments: The authors would like to acknowledge the Hefei Urban Planning & Design Institute and the Anhui Road & Bridge Engineering Group Co., Ltd., for providing detailed information about the asymmetric construction procedure.

Conflicts of Interest: The authors declare no conflict of interest.

References

1. Klar, A.; Vorster, T.E.B.; Soga, K.; Mair, R.J. Soil—Pipe Interaction Due to Tunnelling: Comparison between Winkler and Elastic Continuum Solutions. *Géotechnique* **2005**, *55*, 461–466. [CrossRef]
2. Vorster, T.E.; Klar, A.; Soga, K.; Mair, R.J. Estimating the Effects of Tunneling on Existing Pipelines. *J. Geotech. Geoenvironmental Eng.* **2005**, *131*, 1399–1410. [CrossRef]
3. Zhang, J.-F.; Chen, J.-J.; Wang, J.-H.; Zhu, Y.-F. Prediction of Tunnel Displacement Induced by Adjacent Excavation in Soft Soil. *Tunn. Undergr. Space Technol.* **2013**, *36*, 24–33. [CrossRef]
4. Zhang, Z.; Huang, M.; Wang, W. Evaluation of Deformation Response for Adjacent Tunnels Due to Soil Unloading in Excavation Engineering. *Tunn. Undergr. Space Technol.* **2013**, *38*, 244–253. [CrossRef]
5. Zhang, Z.; Zhang, M.; Zhao, Q. A Simplified Analysis for Deformation Behavior of Buried Pipelines Considering Disturbance Effects of Underground Excavation in Soft Clays. *Arab. J. Geosci.* **2015**, *8*, 7771–7785. [CrossRef]
6. Liang, R.; Xia, T.; Huang, M.; Lin, C. Simplified Analytical Method for Evaluating the Effects of Adjacent Excavation on Shield Tunnel Considering the Shearing Effect. *Comput. Geotech.* **2017**, *81*, 167–187. [CrossRef]
7. Liang, R.; Wu, W.; Yu, F.; Jiang, G.; Liu, J. Simplified Method for Evaluating Shield Tunnel Deformation Due to Adjacent Excavation. *Tunn. Undergr. Space Technol.* **2018**, *71*, 94–105. [CrossRef]
8. Han, J.; Zhao, W.; Jia, P.; Guan, Y.; Chen, Y.; Jiang, B. Risk Analysis of the Opening of Shield-Tunnel Circumferential Joints Induced by Adjacent Deep Excavation. *J. Perform. Constr. Facil.* **2018**, *32*, 04017123. [CrossRef]

9. Sun, H.; Chen, Y.; Zhang, J.; Kuang, T. Analytical Investigation of Tunnel Deformation Caused by Circular Foundation Pit Excavation. *Comput. Geotech.* **2019**, *106*, 193–198. [CrossRef]
10. Xu, R.; Shen, S.; Dong, M.; Cheng, K. A Simplified Calculation Method for Vertical Displacement of Shield Tunnel Caused by Adjacent Excavation. *Geotech. Geol. Eng.* **2021**, *39*, 2269–2286. [CrossRef]
11. Lin, Y.L.; Cheng, X.M.; Yang, G.L.; Li, Y. Seismic response of a sheet-pile wall with anchoring frame beam by numerical simulation and shaking table test. *Soil Dyn. Earthq. Eng.* **2018**, *115*, 352–364. [CrossRef]
12. Lin, Y.L.; Cheng, X.M.; Yang, G.L. Shaking table test and numerical simulation on a combined retaining structure response to earthquake loading. *Soil Dyn. Earthq. Eng.* **2018**, *108*, 29–45. [CrossRef]
13. Lin, Y.L.; Yang, G.L.; Yang, X.; Zhao, L.H.; Shen, Q.; Qiu, M.M. Response of gravity retaining wall with anchoring frame beam supporting a steep rock slope subjected to earthquake loading. *Soil Dyn. Earthq. Eng.* **2017**, *92*, 633–649. [CrossRef]
14. Ng, C.W.W.; Shi, M.J.; Mašín, M.D.; Sun, M.H.; Lei, G.H. Influence of Sand Density and Retaining Wall Stiffness on the Three-Dimensional Responses of a Tunnel to Basement Excavation. *Can. Geotech. J.* **2015**, *52*, 1811–1829. [CrossRef]
15. Huang, X.; Huang, H.; Zhang, D. Centrifuge Modelling of Deep Excavation over Existing Tunnels. *Proc. Inst. Civ. Eng. Geotech. Eng.* **2014**, *167*, 3–18. [CrossRef]
16. Liu, G.B.; Huang, P.; Shi, J.W.; Ng, C.W.W. Performance of a Deep Excavation and Its Effect on Adjacent Tunnels in Shanghai Soft Clay. *J. Perform. Constr. Facil.* **2016**, *30*, 04016041. [CrossRef]
17. Chang, C.-T.; Sun, C.-W.; Duann, S.W.; Hwang, R.N. *Response of a Taipei Rapid Transit System ŽTRTS/Tunnel to Adjacent Excavation*; Elsevier: Oxfprd, UK, 2001; Volume 16, pp. 151–158.
18. Sharma, J.S.; Hefny, A.M.; Zhao, J.; Chan, C.W. Effect of Large Excavation on Deformation of Adjacent MRT Tunnels. *Tunn. Undergr. Space Technol.* **2001**, *16*, 93–98. [CrossRef]
19. Chen, R.; Meng, F.; Li, Z.; Ye, Y.; Ye, J. Investigation of Response of Metro Tunnels Due to Adjacent Large Excavation and Protective Measures in Soft Soils. *Tunn. Undergr. Space Technol.* **2016**, *58*, 224–235. [CrossRef]
20. Meng, F.; Chen, R.; Xu, Y.; Wu, H.; Li, Z. Centrifuge Modeling of Effectiveness of Protective Measures on Existing Tunnel Subjected to Nearby Excavation. *Tunn. Undergr. Space Technol.* **2021**, *112*, 103880. [CrossRef]
21. Chen, S.; Cui, J.; Liang, F. Centrifuge Model Investigation of Interaction between Successively Constructed Foundation Pits. *Appl. Sci.* **2022**, *12*, 7975. [CrossRef]
22. Lin, Y.L.; Li, Y.X.; Zhao, L.H.; Yang, T.Y. Investigation on the seismic response of a three-stage soil slope supported by the anchor frame structure. *J. Cent. South Univ.* **2020**, *27*, 1290–1305. [CrossRef]
23. Lin, Y.L.; Lu, L.; Yang, G.L. Seismic behavior of a single-form lattice anchoring structure and a combined retaining structure supporting soil slope: A comparison. *Environ. Earth Sci.* **2020**, *79*, 78. [CrossRef]
24. Lin, Y.L.; Zhao, L.H.; Yang, T.Y.; Yang, G.L.; Chen, X.B. Investigation on seismic behavior of combined retaining structure with different rock shapes. *Struct. Eng. Mech.* **2020**, *73*, 599–612.
25. Zhang, J.; Xie, R. Effect of Foundation Pit With Different Support and Excavation Methods on Adjacent Buried Hydrogen Pipe. *J. Press. Vessel Technol.* **2021**, *143*, 054502. [CrossRef]
26. Zhou, F.; Zhou, P.; Li, J.; Lin, J.; Ge, T.; Deng, S.; Ren, R.; Wang, Z. Deformation Characteristics and Failure Evolution Process of the Existing Metro Station under Unilateral Deep Excavation. *Eng. Fail. Anal.* **2022**, *131*, 105870. [CrossRef]
27. Wang, C.; Sun, H.; Zhang, J.; Lu, Y. Influence of Foundation Pit Excavation on Tunnels at Different Locations. *Shock. Vib.* **2022**, *2022*, 4282253. [CrossRef]
28. Yang, Q.-R.; Li, M.-G.; Chen, J.-J. Influence of a Flexible Retaining Wall on Performance of an Adjacent Deep Excavation. *KSCE J. Civ. Eng.* **2022**, *26*, 661–672. [CrossRef]
29. Liu, B.; Lin, H.; Chen, Y.; Liu, J.; Guo, C. Deformation Stability Response of Adjacent Subway Tunnels Considering Excavation and Support of Foundation Pit. *Lithosphere* **2022**, *2022*, 7227330. [CrossRef]
30. Chen, T.; Zhou, K.; Wei, J.; Liu, X.C.; Lin, Y.L.; Zhang, J.; Shen, Q. Analysis on the excavation influence of triangular-distribution tunnels for the wind pavilion group of a metro station. *J. Cent. South Univ.* **2020**, *27*, 3852–3874. [CrossRef]
31. Liao, S.-M.; Wei, S.-F.; Shen, S.-L. Structural Responses of Existing Metro Stations to Adjacent Deep Excavations in Suzhou, China. *J. Perform. Constr. Facil.* **2016**, *30*, 04015089. [CrossRef]
32. Li, M.-G.; Wang, J.-H.; Chen, J.-J.; Zhang, Z.-J. Responses of a Newly Built Metro Line Connected to Deep Excavations in Soft Clay. *J. Perform. Constr. Facil.* **2017**, *31*, 04017096. [CrossRef]